Contents of this file

This document includes seven figures to supplement the main text.

Introduction

Figures S1 – S4 show the location of the observation-based velocity grid points (blue) and of the selected 'transport' points (red) from the reanalysis in Davis Strait (S1), Fram Strait (S2), the Barents Sea Opening (S3) and Bering Strait (S4).

5 Additionally, S1 includes the reanalysis grid for meridional velocities (the v-grid) in black. Points located on the intersections of grid lines contain meridional velocities, points located in the space between grid lines contain zonal velocities. These figures are supplementary to section 3 in the main text. The red points are chosen such that the absolute distance to the observation-based grid is minimized.

10 Figure S5 is derived from the reanalysis (C-GLORS version7) in support of section 3. Here we show that the temperature transport due to 'transient' (sub-monthly scale) eddies is small compared to the temperature transport from the stationary (monthly scale) circulation. The temperature transport due to transient eddies is equal to

$$\overline{v_2' \cdot \theta'} = \overline{v_2 \cdot \theta} - \overline{v_2} \cdot \overline{\theta}.$$

The primed quantities are the deviation of daily velocity and potential temperature from the monthly averages of the respective

15 fields. The overbar denotes monthly averages. The first term on the right-hand side is the product of daily velocity and daily potential temperature fields averaged over each month. This represents the 'total' temperature transport. The second term is the temperature transport associated with the stationary circulation. Figure S5 shows that we do not introduce a considerable error to the reanalysis-based temperature transports by using monthly averages instead of daily data, since the temperature transport due to transient eddies is small compared to the 'stationary' temperature transport. Averaged over the study period,

20 the temperature transport due to transient eddies contributes – 12.5 % to the total temperature transport in Davis Strait, 0.01 % in Fram Strait, 0.6 % in the Barents Sea Opening, 7.1 % in Bering Strait and 0.8 % to the net temperature transport into the Arctic Ocean.

Figures S6 and S7 show volume and temperature transport anomalies (with respect to the 2000 – 2013 climatology) across 70°

25 N derived solely from the reanalysis but in three different ways: The first option is to use fields of vertically integrated meridional and zonal volume and temperature transports, which are available on the model-native grid from post-processing ('post-proc.', grey line in Fig. S6 - S7). The second option is to use the integrated transport fields which have been interpolated onto a regular latitude/longitude grid ('Interp.', salmon colored). The last possibility is to calculate the volume and temperature transports from fields of velocity and temperature on the model native grid as described in the main text ('With SSH' in orange

30 and 'Without SSH' in black). As a reference, Fig. S6 also includes the net volume transport anomalies derived from the surface

freshwater flux (positive upward so that it should equal the oceanic volume transport, 'FW up' in blue). The freshwater flux is given on the interpolated grid and is converted to a volume flux using $\rho = 1000$ kg/m³. The lines have been temporally smoothed by applying a 12-month running mean. For calculating the transports through 70° N on the model native grid, we employ the same algorithm as described in the main text for finding appropriate native grid points closest to 70° N (or more precisely, 69.875° N, which is a latitude circle on the interpolated grid).

The comparisons in Fig. S6 and S7 show that calculating the transports based on velocity and temperature fields on the model native grid yields the most reliable results: For one, the mean volume and heat transport estimates are closer to the net transports from the mooring-derived dataset (- 0.15 ± 0.06 Sv and 153 ± 44 TW, see Sect. 4.1) when derived directly from temperature and velocity fields (- 0.14 ± 0.18 Sv and 180 ± 40 TW both with and without the transports through the sea surface height layer) compared to the post-processed fields (native grid: + 0.3 ± 8.9 Sv and 240 ± 110 TW, interpolated grid: - 0.83 ± 2.29 Sv and 246 ± 56 TW). Second, the amplitude of monthly variability is unrealistically high in the post-processed time series. This comparison was conducted for the previous release of the reanalysis (C-GLORSv5), which was originally the basis of this study, but post-processing has not changed between v5 and v7, so the conclusion still holds true for the newer version.
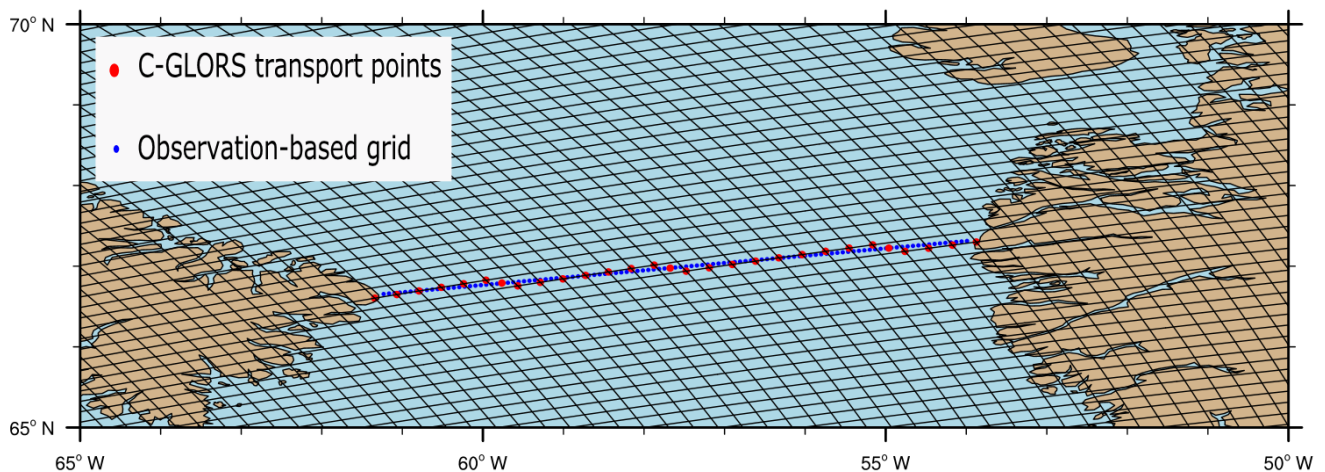
Figure S1 – 'Transport points' in Davis Strait and observation-based datapoints. Black lines show the reanalysis grid of meridional velocities (v-grid).
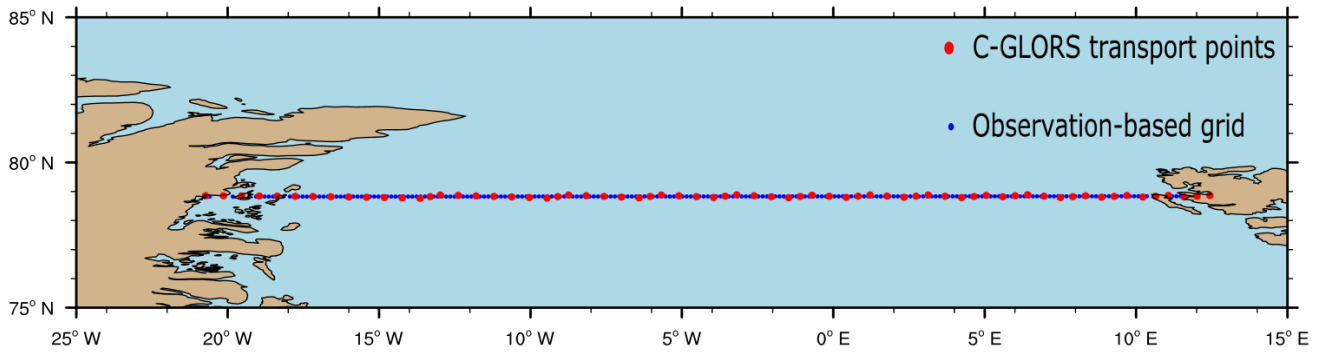
Figure S2 – 'Transport points' in Fram Strait and observation-based datapoints.
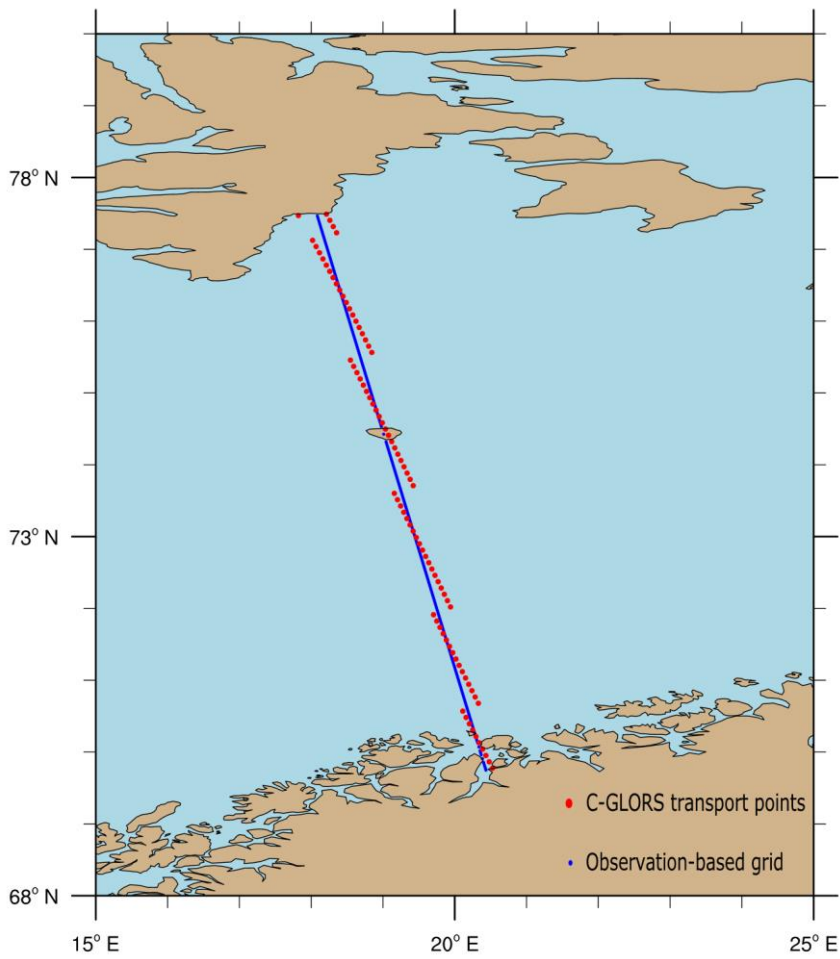
10

Figure S3 – 'Transport points' in the Barents Sea Opening and observation-based datapoints.
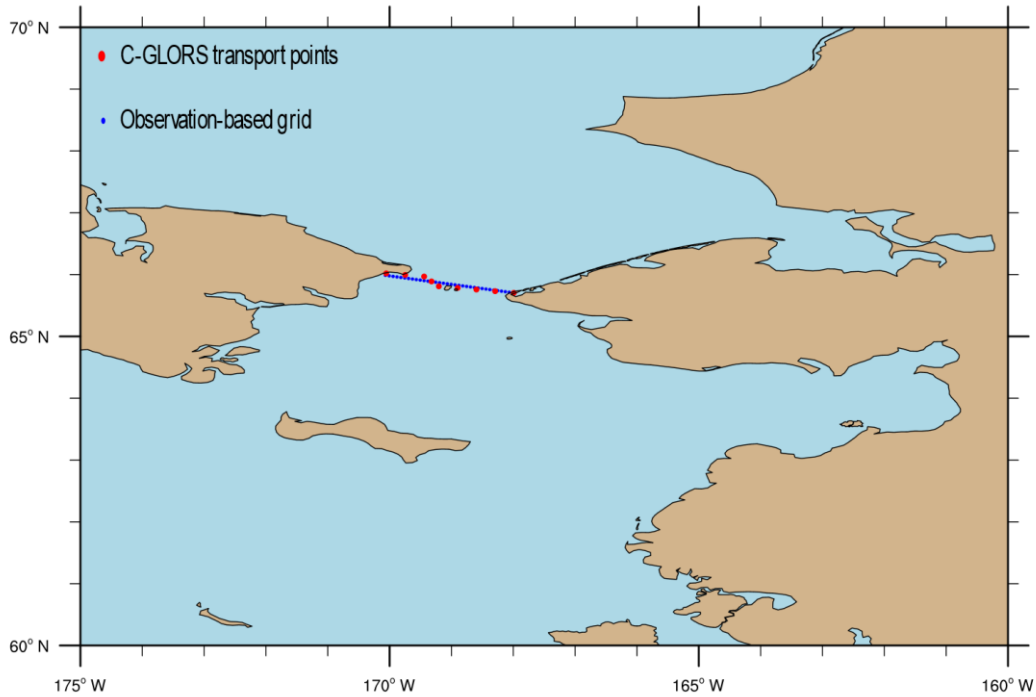
Figure S4 – 'Transport points' in Bering Strait and observation-based datapoints.
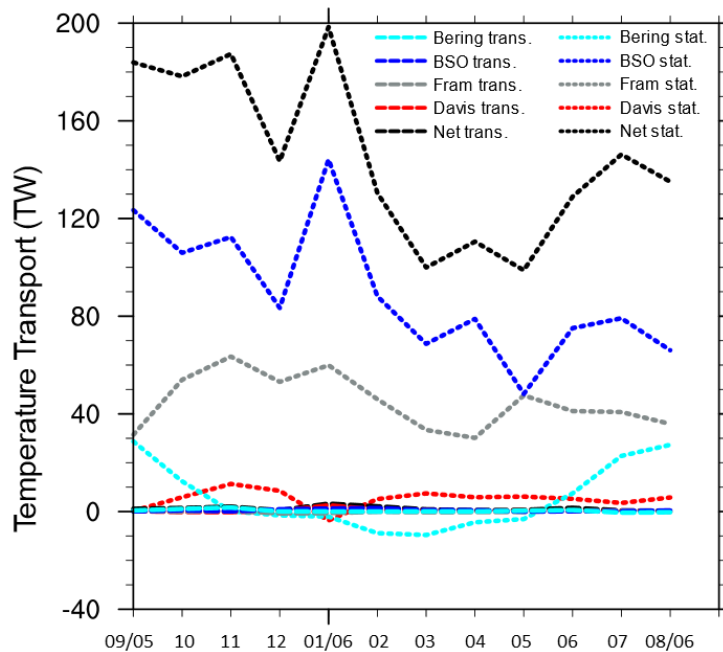
Figure S5 - Temperature transports through each strait and net temperature transport into the Arctic Ocean split up into the contributions from the 'stationary circulation' (dotted) and 'transient eddies' (dashed).
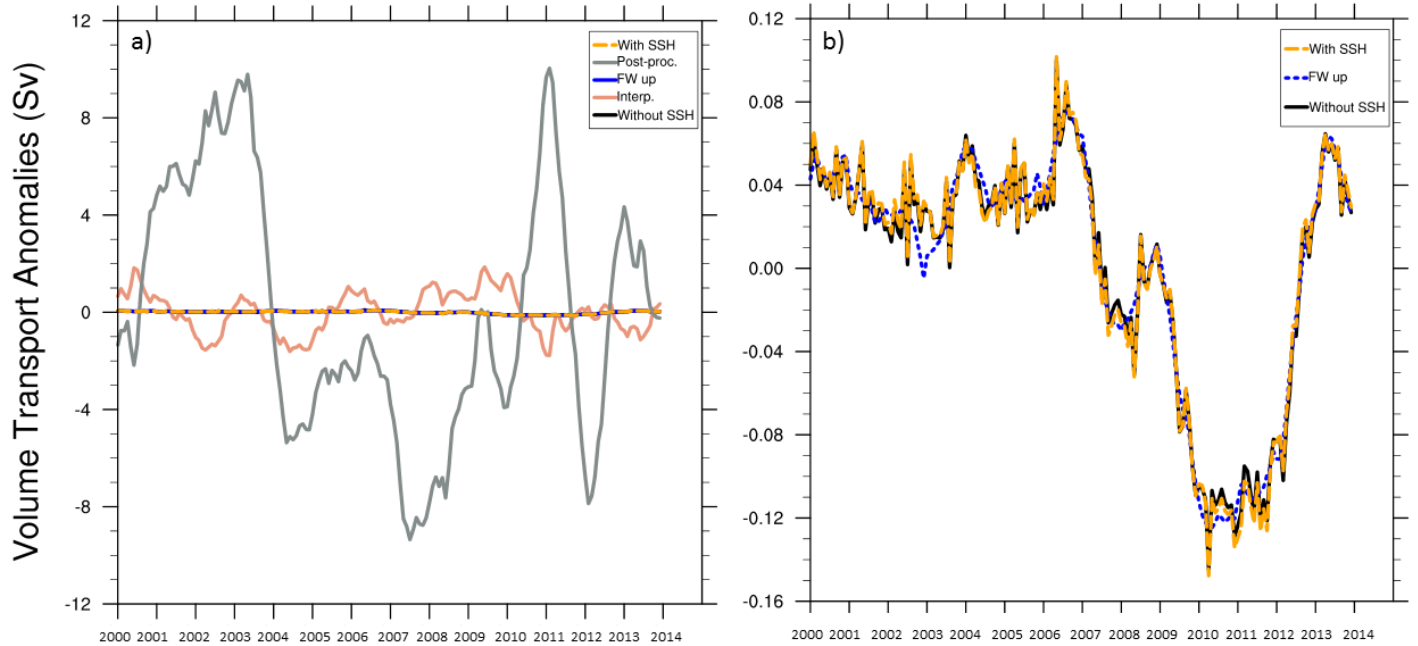
Figure S6 – Volume transport anomalies through 70° N based on the monthly climatology for the period January 2000 to December 2013. In (b), the transports from post-processing are omitted to highlight the good agreement between the transports derived from the velocities on the native grid and the freshwater flux. Note the different scales in (a) and (b).
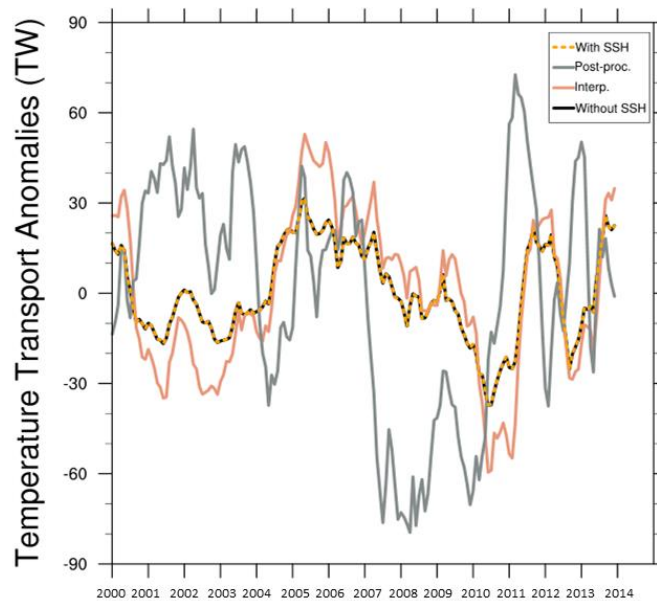
Figure S7 – Temperature transport anomalies through 70° N based on the monthly climatology for the period January 2000 to December 2013.